

# Dynamical thermalization in time-dependent billiards

Cite as: Chaos **29**, 103122 (2019); <https://doi.org/10.1063/1.5120023>

Submitted: 15 July 2019 . Accepted: 24 September 2019 . Published Online: 11 October 2019

Matheus Hansen , David Ciro , Iberê L. Caldas , and Edson D. Leonel 



View Online



Export Citation



CrossMark

AIP Author Services  
English Language Editing



# Dynamical thermalization in time-dependent billiards

Cite as: Chaos 29, 103122 (2019); doi: 10.1063/1.5120023

Submitted: 15 July 2019 · Accepted: 24 September 2019 ·

Published Online: 11 October 2019



View Online



Export Citation



CrossMark

Matheus Hansen,<sup>1,a)</sup> David Ciro,<sup>2</sup> Iberê L. Caldas,<sup>1</sup> and Edson D. Leonel<sup>3</sup>

## AFFILIATIONS

<sup>1</sup>Instituto de Física, Universidade de São Paulo, São Paulo CEP 05508-090, SP, Brazil

<sup>2</sup>Instituto de Astronomia Geofísica e Ciências Atmosféricas, Universidade de São Paulo, São Paulo CEP 05508-090, SP, Brazil

<sup>3</sup>Departamento de Física, UNESP, Rio Claro CEP 13506-900, SP, Brazil

<sup>a)</sup>Electronic mail: [mathehansen@gmail.com](mailto:mathehansen@gmail.com)

## ABSTRACT

Numerical experiments of the statistical evolution of an ensemble of noninteracting particles in a time-dependent billiard with inelastic collisions reveals the existence of three statistical regimes for the evolution of the speed ensemble, namely, diffusion plateau, normal growth/exponential decay, and stagnation. These regimes are linked numerically to the transition from Gauss-like to Boltzmann-like speed distributions. Furthermore, the different evolution regimes are obtained analytically through velocity-space diffusion analysis. From these calculations, the asymptotic root mean square of speed, initial plateau, and the growth/decay rates for an intermediate number of collisions are determined in terms of the system parameters. The analytical calculations match the numerical experiments and point to a dynamical mechanism for “thermalization,” where inelastic collisions and a high-dimensional phase space lead to a bounded diffusion in the velocity space toward a stationary distribution function with a kind of “reservoir temperature” determined by the boundary oscillation amplitude and the restitution coefficient.

Published under license by AIP Publishing. <https://doi.org/10.1063/1.5120023>

Billiards are systems that represent the background of the statistical physics and the theory of dynamical systems. Because of their rich dynamical properties and easy understanding, the billiard models can be applied in order to describe several problems in many different branches of physics. In this work, we use the billiard theory to study the statistical evolution of the speeds from an ensemble of noninteracting particles in a time-dependent billiard when inelastic collisions are observed. We present numerical and analytical explanations for all stages of the speed ensemble evolution until the thermalization state is reached. We also demonstrate that this final state of thermalization, actually, works as a kind of reservoir temperature, which is characterized by the boundary parameters of the time-dependent system.

## I. INTRODUCTION

The Loskutov-Ryabov-Akinshin (LRA) conjecture<sup>1</sup> was proposed as an attempt to foresee what would happen to the behavior of the average velocity for an ensemble of particles in a time dependent billiard<sup>2,3</sup> whenever the shape and characteristics of the phase space of the corresponding static version of the billiard was known.

Chaos in the phase space for the dynamics of a particle in a billiard with a static boundary was claimed by the conjecture to be a sufficient condition to produce unlimited energy growth, also known as Fermi acceleration,<sup>4</sup> of the particles when a time perturbation to the boundary was introduced. The conjecture was tested in a number of billiards being therefore validated.<sup>5,6</sup> A counterexample of such conjecture was observed in an elliptic billiard,<sup>2,3</sup> whose structure is integrable in the static form, but that presents an unlimited diffusion of energy when a time-dependence is introduced on the billiard boundary.

The physics behind the unlimited energy growth is understood and is mainly related to the diffusion of velocities as a function of time.<sup>7-10</sup> Different regimes of growth are related to different shapes of the speed distribution function. The counterintuitive fact that Hamiltonian dynamics may lead to an unlimited energy growth in chaotic billiards comes from the higher dimension of the dynamical system, and such a growth appears to contradict what is expected from thermodynamics. However, this only states that there is not a well-defined temperature for the moving boundary, which works here as the energy reservoir; i.e., the wall is not in a thermodynamic equilibrium. In a regular situation, a gas of noninteracting particles with an initial low temperature  $T_0$  will increase its energy if

introduced in a, previously empty, recipient with walls at ambient temperature  $T_a > T_0$ . The opposite will happen if the gas is at an initially larger temperature  $T_0 > T_a$ .<sup>11</sup> This thermalization process, in general, manifests as a monotonic change in temperature as time advances, leading to an asymptotic state of thermal equilibrium.

In contrast, consider a conservative chaotic billiard with an oscillating boundary, such that unlimited energy growth is observed. Since the billiard energy is essentially kinetic, the growth of energy leads also to the growth of the temperature. The type of interaction of the particle with the boundary is the reason of such behavior. Elastic collisions preserve both momentum and kinetic energy in the moving referential frame of the boundary, which does not imply conservation of energy for the inertial frame of the gas center of mass, leading to the unlimited energy growth of the ensemble of particles.

On the other hand, inelastic collisions preserve only momentum, and the dissipation introduced produces drastic topological changes in the phase space. When inelastic collisions are taken into account, the Liouville measure is no longer preserved, and attractors can develop in the phase space.<sup>12</sup> Considering that the attractor is located at finite values of the velocity, and its basins of attraction contain most of the phase space, it is clear that the individual trajectories will converge to the attractor, and the average speed will saturate, leading to a sort of thermodynamical equilibrium for the perturbed billiard.

Until now, important results have been obtained in the characterization of the unbounded energy evolution for particles in chaotic billiards. Our contribution in this context is the statistical description of the evolution to a final equilibrium and the close connection of this behavior with thermal equilibrium. To our knowledge, this problem has not been addressed elsewhere and offers a significant analogy between dynamical and thermal equilibrium.

In this paper, we discuss the dynamics of an ensemble of particles moving in an oval billiard with a periodically oscillating boundary. We consider inelastic collisions of the particles with the boundary and explore the behavior of the root mean square of speed considering the shape of the probability distribution function of the speeds. Then, we show that the presence of dissipation leads the system toward an asymptotic stationary state, which, with basis on its statistical properties, we argue is a dynamical equivalent of a thermodynamical equilibrium.

The paper is organized as follows. In Sec. II, we discuss the equations that compose the billiard model with a time-dependent boundary. In Sec. III, we show the statistical analysis of the speeds and the diffusion process in the system. In Sec. IV, we present an analytical derivation of the time evolution of the root mean square of the speeds in terms of the control parameters of the problem. In Sec. V, we offer a connection between the asymptotic dynamics of dissipative time-dependent billiards and the concept of thermalization. Finally, in Sec. VI, we present our conclusions and final remarks.

## II. THE TIME-DEPENDENT BILLIARD

We start considering a time-dependent oval billiard<sup>13</sup> with a boundary described in a polar form as

$$R_b(\theta, \epsilon, t, a, p) = 1 + \epsilon [1 + a \cos(t)] \cos(p\theta), \quad (1)$$

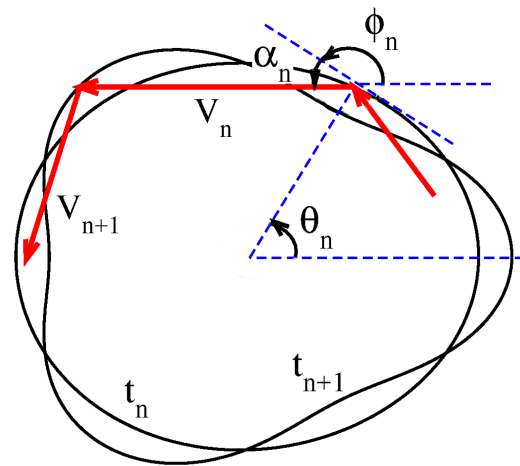


FIG. 1. Sketch of two consecutive collisions (red line) of a particle in a time-dependent oval-billiard with  $a = 0.9$ ,  $\epsilon = 0.08$ , and  $p = 3$ .

where  $R_b$  is the boundary radial coordinate,  $\theta$  is the polar angle,  $\epsilon$  measures the oval deformation,  $t$  is the time,  $a$  is the boundary oscillation amplitude, and  $p$  is a positive integer.<sup>14</sup>

The trajectory of a particle inside of the billiard can be described using a nonlinear four-dimensional mapping  $H : \mathbb{R}^4 \rightarrow \mathbb{R}^4$ , such that  $(\theta_{n+1}, \alpha_{n+1}, V_{n+1}, t_{n+1}) = H(\theta_n, \alpha_n, V_n, t_n)$ . The angle  $\alpha_n$  is measured between the particle trajectory and the tangent line to the boundary at  $(\theta_n, t_n)$ , after the  $n$ th collision with the wall, and  $V_n = |\vec{V}_n|$  is the velocity magnitude. Figure 1 shows in red a sketch of a typical trajectory of a particle at different times in the model.

Given that there are no additional potentials inside the billiard, each particle moves with constant speed along a straight line between collisions. The radial position of the particle is given by  $R_p(t) = \sqrt{X_p^2(t) + Y_p^2(t)}$ , where  $X_p(t)$  and  $Y_p(t)$  are the rectangular coordinates at time  $t$ , which are given by

$$X_p(t) = X(\theta_n, t_n) + |\vec{V}_n| \cos(\mu)[t - t_n], \quad (2)$$

$$Y_p(t) = Y(\theta_n, t_n) + |\vec{V}_n| \sin(\mu)[t - t_n], \quad (3)$$

with  $\mu = (\alpha_n + \phi_n)$  and  $\phi = \arctan(Y'(\theta, t)/X'(\theta, t))$ , where  $Y'(\theta, t) = dY/d\theta$  and  $X'(\theta, t) = dX/d\theta$ .

The new dynamical variable  $\theta$  at collision  $n + 1$  is obtained through the numerical solution of the implicit equation  $R_b(\theta_{n+1}, t_{n+1}) = R_p(\theta_{n+1}, t_{n+1})$ , with the time  $t_{n+1}$  given by

$$t_{n+1} = t_n + \frac{\sqrt{\Delta X_p^2 + \Delta Y_p^2}}{|\vec{V}_n|}, \quad (4)$$

where  $\Delta X_p = X_p(\theta_{n+1}, t_{n+1}) - X(\theta_n, t_n)$  and  $\Delta Y_p = Y_p(\theta_{n+1}, t_{n+1}) - Y(\theta_n, t_n)$ .

The reflection laws for each collision of the particle with the boundary can be obtained by applying conservation of momentum in an instantly inertial frame where the contact point of the billiard

is at rest. In our case, the reflection laws are

$$\begin{aligned} \vec{V}'_{n+1} \cdot \vec{T}_{n+1} &= \xi \vec{V}'_n \cdot \vec{T}_{n+1}, \\ \vec{V}'_{n+1} \cdot \vec{N}_{n+1} &= -\kappa \vec{V}'_n \cdot \vec{N}_{n+1}, \end{aligned}$$

where  $\vec{T}_{n+1} = \cos(\phi_{n+1})\hat{i} + \sin(\phi_{n+1})\hat{j}$  and  $\vec{N}_{n+1} = -\sin(\phi_{n+1})\hat{i} + \cos(\phi_{n+1})\hat{j}$  are the tangent and normal unit vectors,  $\vec{V}'$  is the particle velocity measured in the noninertial frame, and  $\xi, \kappa \in [0, 1]$  are the tangent and normal restitution coefficients, respectively.

After collision  $n + 1$ , the tangent and normal components of the velocity are

$$\vec{V}_{n+1} \cdot \vec{T}_{n+1} = (1 - \xi)\vec{V}_b \cdot \vec{T}_{n+1} + \xi \vec{V}_n \cdot \vec{T}_{n+1}, \quad (5)$$

$$\vec{V}_{n+1} \cdot \vec{N}_{n+1} = (1 + \kappa)\vec{V}_b \cdot \vec{N}_{n+1} - \kappa \vec{V}_n \cdot \vec{N}_{n+1}, \quad (6)$$

where

$$\vec{V}_b = \frac{dR_b(t)}{dt} \Big|_{t_{n+1}} [\cos(\theta_{n+1})\hat{i} + \sin(\theta_{n+1})\hat{j}] \quad (7)$$

is the boundary velocity at time  $t_{n+1}$ . The magnitude of the particle velocity after collision  $n + 1$  is

$$|\vec{V}_{n+1}| = \sqrt{[\vec{V}_{n+1} \cdot \vec{T}_{n+1}]^2 + [\vec{V}_{n+1} \cdot \vec{N}_{n+1}]^2}, \quad (8)$$

and the reflection angle  $\alpha_{n+1}$  is

$$\alpha_{n+1} = \arctan \left[ \frac{\vec{V}_{n+1} \cdot \vec{N}_{n+1}}{\vec{V}_{n+1} \cdot \vec{T}_{n+1}} \right]. \quad (9)$$

### III. SYSTEM EVOLUTION AND SPEED DISTRIBUTION

In contrast to the static situation, in a time-dependent billiard, particles can gain or lose energy upon interaction with the moving boundary. For an ensemble of particles, the individual gains and losses do not necessarily compensate and the mean energy can change in time. The details of this process can be relevant to understand rates of change in the energy, but here, we start with a simple heuristic analysis that reveals the broad aspects of the energy evolution.

First of all, consider that the mean quadratic speed changes by an amount  $\psi$  after each collision. We consider here a situation in which there is a small fractional loss of energy after each collision characterized by some restitution coefficient  $\gamma < 1$ , and then the mean energy after a collision  $n$  satisfies approximately

$$\overline{V_{n+1}^2} = \gamma(\overline{V_n^2} + \psi). \quad (10)$$

This dynamical system has a stable equilibrium when the fractional loss compensates exactly the energy gain after collision. Regardless of the initial configuration, after many collisions, it is expected that the quadratic speed  $\overline{V_{n+1}^2}$  will approach a stagnation value  $V_{sta}$  given by

$$V_{sta} = \sqrt{\frac{\gamma\psi}{1-\gamma}}. \quad (11)$$

Notice for elastic collisions  $\gamma \rightarrow 1$ , the stagnation speed diverges, which is consistent with the phenomenon of Fermi acceleration, where there is an unlimited growth of energy as the time evolves.<sup>7,10,15</sup>

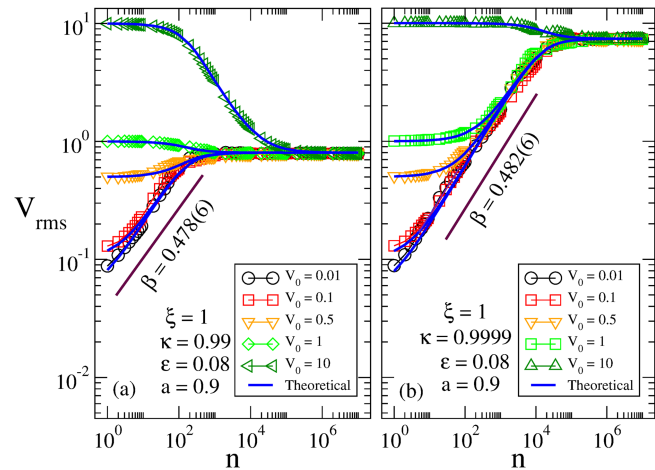


FIG. 2. (a) and (b) Plot for  $V_{rms}$  vs  $n$  for different initial speeds and parameters.

To illustrate numerically the stagnation process, we consider the root mean square of the speed distribution for an ensemble of non-interacting particles in the time-dependent oval-billiard described in Sec. I. To reduce numerical fluctuations, in addition to the instantaneous ensemble average, we consider also the time average of the quadratic velocity for the ensemble of particles,

$$V_{rms} = \sqrt{\frac{1}{M} \sum_{i=1}^M \frac{1}{n+1} \sum_{j=0}^n |\vec{V}_{i,j}|^2}, \quad (12)$$

where  $\vec{V}_{i,j}$  is the velocity of the  $i$ th particle after collision  $j$ . The first summation is made over an ensemble of different initial conditions randomly chosen in  $t \in [0, 2\pi]$ ,  $\alpha \in [0, \pi]$ , and  $\theta \in [0, 2\pi]$ , where all the particles have the same initial speed  $V_0$ , while the second summation is made over the individual orbits. In our simulations, we considered an ensemble of  $M = 10^6$  particles colliding  $10^7$  times with the boundary.

The numerical evolution of  $V_{rms}$  is presented in Figs. 2(a) and 2(b) for two different restitution coefficients  $\kappa$  and various initial configurations with different  $V_0$ . These curves in Fig. 2 exhibit three different evolution stages for each initial speed. Initially, for speeds around the maximum speed of the boundary  $V_{max} = a\epsilon$ ,  $V_{rms}$  has a plateau whose extension depends on the initial speed of the particles. After a first crossover, the system enters the growth regime following a power law with exponent  $\beta \sim 1/2$  of the number of collisions  $n$ . Finally, a second crossover is observed after which the  $V_{rms}$  saturates at  $V_{sta}$ . It can also be observed that when  $V_0 \gg a\epsilon$ ,  $V_{rms}$  decays exponentially to the stagnation regime in agreement with the heuristic discussion in Sec. III.

However, to understand in a more detailed fashion the growth rates and transition values, we need to take into account the diffusion of particles in the velocity space  $(V_x, V_y)$ .<sup>16</sup> At the initial stage, all particles exist on a circle of radius  $V_0$ . After a collision, each particle jumps by a small amount  $(\delta V_x, \delta V_y)$  in some direction. Provided there are more available states in the velocity space outside the circle

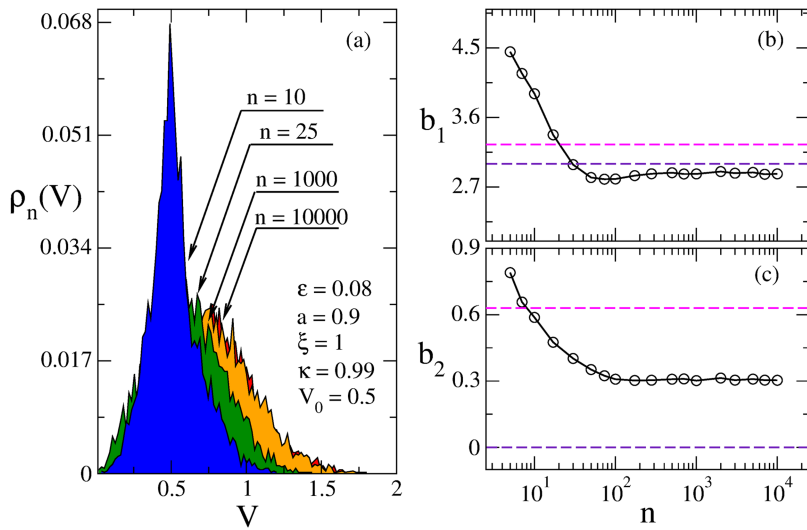


**FIG. 3.** (a) Plot of the evolution of the speed distribution function  $\rho_n(V)$  for an ensemble of  $10^6$  particles, with initial speed  $V_0 = 0.5$ , after different number of collisions  $n$  and (b) and (c) plot of the measurement of the kurtosis  $b_1$  and skewness  $b_2$  (black curve in both figures), respectively, for the speed distribution function after different number of collisions. The purple and pink dashed lines are the values for the kurtosis and skewness for the normal and two-dimensional Maxwell-Boltzmann distributions, respectively.

than inside, the probability of particles moving outside the circle is larger than inward. This small imbalance leads to a growth in the  $V_{rms}$  of the ensemble when the initial radius  $V_0$  is below  $V_{sta}$ . However, the initial growth rate is very small because the initial distribution of particles has to relax toward a Gaussian distribution before exhibiting the usual growth rate for a random walk  $\beta_{RW} = 1/2$ . Such a relaxation process results in an initial plateau that is longer for larger initial speeds. For large initial velocities  $V_0 > V_{sta}$ , the initial plateau occurs in the same fashion, but the probability of moving inward is larger because with each collision, the particles must give up an amount of energy proportional to  $V^2$ . Although there are also losses for small velocities, the diffusion there dominates because the characteristic value of  $\delta V^2$  is larger than the energy lost after each collision.

In Fig. 3(a), for the same parameters of Fig. 2(a) and  $V_0 = 0.5$ , we present the evolution of the speed distribution function  $\rho_n(V)$  as the number of collisions increases. The 10th collision corresponds to the plateau region of Fig. 2(a) (for  $V_0 = 0.5$ ) where a spreading Gauss-like distribution preserves its mean around the initial speed until it reaches  $V = 0$  at the left side. At the 25th collision, the system is in the growth regime, and finally, for the 1000th and 10 000th collisions, the speed distribution does not change appreciably because the system reached its stagnation regime. Thus, comparing Figs. 2(a) and 3(a), we can follow, for  $V_0 = 0.5$ , the  $V_{rms}$  and  $\rho_n(V)$  evolution as  $n$  increases.

In order to characterize quantitatively the shape evolution of the speed distribution with the number of collisions, we calculated the kurtosis  $b_1$  and skewness  $b_2$  for  $\rho_n(V)$  as functions of the number of collisions with usual definitions,<sup>17</sup> given by

$$b_1 = \frac{1}{M} \sum_{i=1}^M \left[ \frac{V_i - \bar{V}}{\sigma} \right]^4, \tag{13}$$

$$b_2 = \frac{1}{M} \sum_{i=1}^M \left[ \frac{V_i - \bar{V}}{\sigma} \right]^3, \tag{14}$$

where  $\sigma_V = \sqrt{\langle V^2 \rangle - \langle V \rangle^2}$ .

Figures 3(b) and 3(c) show the evolution of  $b_1$  and  $b_2$  for the speed distribution function presented in Fig. 3(a). This figure also shows the values of  $b_1$  and  $b_2$  for the normal (purple dashed line) and a two-dimensional Maxwell-Boltzmann (pink dashed line) distributions, which differ from ours because of the stochastic nature of their associated processes.

Notice that after  $\rho_n(V)$  reaches the stagnation regime (about 100 collisions), the kurtosis measurement ( $b_1 \approx 2.87$ ) is close to that of a normal distribution, while the skewness measurement ( $b_2 \approx 0.30$ ) is an intermediary value between the normal and the Maxwell-Boltzmann distributions.

#### IV. KINETIC ANALYSIS

Consider that the quadratic speed of a single particle,  $\tilde{V}^2$ , changes by an amount  $\psi(\alpha, \theta, t, V)$  after colliding with the boundary at position  $\theta$  with incidence angle  $\alpha$  at time  $t$ ,

$$\tilde{V}^2(\alpha, \theta, t, V) = V^2 + \psi(\alpha, \theta, t, V), \tag{15}$$

where  $V^2$  and  $\tilde{V}^2$  are the quadratic speeds before and after collision. In an ensemble of  $M$  particles, there are approximately  $M \mathcal{F}_n(\alpha, \theta, t, V) d\alpha d\theta dt dV$  particles with variable  $x$  between  $x$  and  $x + dx$ , where  $x = \{\alpha, \theta, V, t\}$ . Then, it is possible to describe the mean quadratic speed after the  $n$ th collision of an ensemble of particles as

$$\overline{V_{n+1}^2} = \overline{V_n^2} + \delta \overline{V_n^2}, \tag{16}$$

where

$$\overline{V_n^2} = \int_0^\infty \int_0^{2\pi} \int_0^{2\pi} \int_0^\pi V^2 \mathcal{F}_n(\alpha, \theta, t, V) d\alpha d\theta dt dV, \tag{17}$$

$$\delta \overline{V_n^2} = \int_0^\infty \int_0^{2\pi} \int_0^{2\pi} \int_0^\pi \psi(\alpha, \theta, t, V) \times \mathcal{F}_n(\alpha, \theta, t, V) d\alpha d\theta dt dV, \tag{18}$$

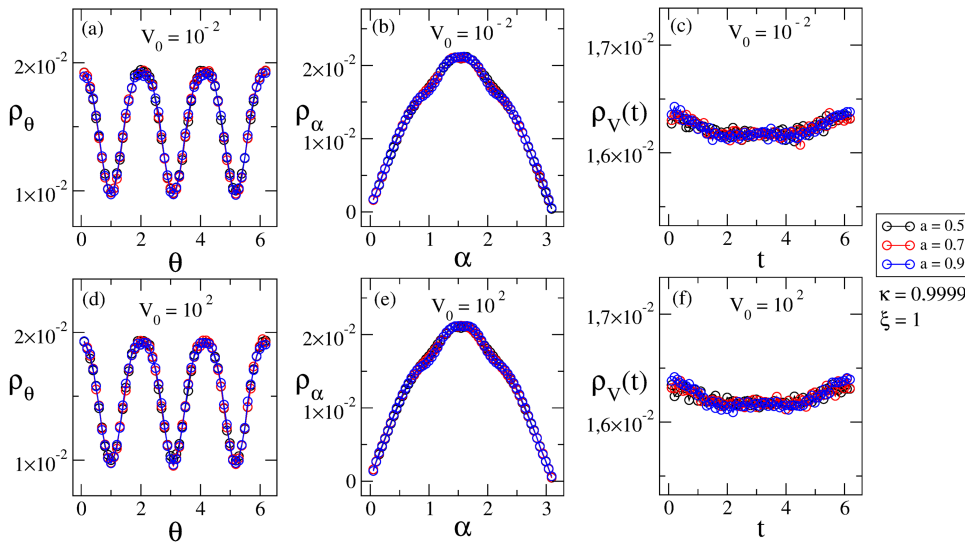


**FIG. 4.** (a), (b), (d), and (e) Plot of the numerical distribution functions  $\rho_\theta(\theta) = \int \bar{F}(\theta, \alpha)d\alpha$  and  $\rho_\alpha(\alpha) = \int \bar{F}(\theta, \alpha)d\theta$ , while (c) and (f) plot of the numerical collision time distribution functions  $\rho_V(t)$  for the time-dependent oval-billiard at various amplitudes of oscillations and two initial speeds. The control parameters are  $\epsilon = 0.08$  and  $p = 3$ .

and  $\mathcal{F}_n(\alpha, \theta, t, V)$  is the full phase-space distribution function after collision  $n$ . In our case, we can factor this distribution as

$$\mathcal{F}_n(\alpha, \theta, t, V) = F(\theta, \alpha)\rho_V(t)\rho_n(V), \tag{19}$$

where  $F(\alpha, \theta)$  are the angle distribution,  $\rho_V(t)$  is the collision time distribution, and  $\rho_n(V)$  is the speed distribution function.

As observed in Figs. 4(a)–4(f), the angles  $F(\alpha, \theta)$  and collision time distributions  $\rho_V(t)$  are almost unaffected by the amplitude of the boundary oscillations  $a$ . Consequently, they are almost independent of the index  $n$  and on the initial speed values. This can be understood in terms of the phase-space projection  $\theta - \alpha$ , which retains important features of the unperturbed problem, which is independent of the velocity of the particles and contains large regular regions with invariant tori that modulate the size of the chaotic region as a function of the angles  $\theta - \alpha$ , in a way consistent with Fig. 4.

On the other hand, as discussed in Sec. III, the speed distribution function  $\rho_n(V)$  [see Fig. 3(a)] depends on both the speed and the index  $n$ .

Using decomposition (19), we want to find an analytical expression that describes the behavior of the root mean square speed shown in Figs. 2(a) and 2(b). As discussed in Ref. 10, to determine the behavior of the mean quadratic speed, it is not necessary to describe the evolution of the global distribution function, but only to know the evolution of its first momenta. Therefore, replacing Eq. (19) in Eq. (17) and defining the partial mean

$$W(V) = \int_0^{2\pi} \int_0^{2\pi} \int_0^\pi \psi(\alpha, \theta, t, V)F(\theta, \alpha)\rho_V(t)d\alpha d\theta dt, \tag{20}$$

we can write a more compact expression for the change of the mean quadratic speed as

$$\delta \overline{V}_n^2 = \int_0^\infty \rho_n(V)W(V)dV. \tag{21}$$

As detailed in Ref. 10, if we make a second-order expansion of the  $W(V)$  around the mean speed  $\overline{V}_n$  of the speed distribution

function  $\rho_n(V)$ , we obtain

$$W(V) \approx W(\overline{V}_n) + W'(\overline{V}_n)(V - \overline{V}_n) + \frac{1}{2}W''(\overline{V}_n)(V - \overline{V}_n)^2. \tag{22}$$

Inserting Eq. (22) in Eq. (21), we obtain an approximation for the change of the mean quadratic speed using the second-order expansion, as follows:

$$\delta \overline{V}_n^2 = W(\overline{V}_n) + \frac{1}{2}W''(\overline{V}_n)(\overline{V}_n^2 - \overline{V}_n^2). \tag{23}$$

Notice also that Eq. (22) is accurate only around the distribution mean. As we get far from the mean value, the approximation becomes poorer. However,  $\rho_n(V)$  in the integrand of Eq. (21) drops for large and small values of the speed, so the integrand is small where the expansion of  $W(V)$  is not accurate. The interested reader can find more details about these approximations in Ref. 10.

Finally, replacing Eq. (23) in Eq. (16), we find a second-order approximation for the mean quadratic speed after collision  $n$ , as follows:

$$\overline{V}_{n+1}^2 = \overline{V}_n^2 + W(\overline{V}_n) + \frac{1}{2}W''(\overline{V}_n)(\overline{V}_n^2 - \overline{V}_n^2). \tag{24}$$

In order to determine the partial mean  $W(V)$ , we first need to find  $\psi(\alpha, \theta, t)$ , which depends on the particular problem. In this case, the equations of the time-dependent oval-billiard lead us to

$$\begin{aligned} \psi(\alpha, \theta, t) &= (\kappa^2 - 1)V^2 \sin^2(\alpha) \\ &+ (1 + \kappa)^2(a\epsilon)^2 \cos^2(p\theta) \sin^2(t) \\ &+ 2V\kappa a\epsilon(1 + \kappa) \sin(\alpha) \cos(p\theta) \sin(t). \end{aligned} \tag{25}$$

Assuming that the collision time distribution  $\rho_V(t)$  is approximately uniform, i.e.,

$$\rho_V(t) = \frac{1}{2\pi}, \tag{26}$$

and replacing Eqs. (25) and (26) in Eq. (20), we obtain

$$W(V) = \eta_1(\kappa^2 - 1)V^2 + \frac{1}{2}(1 + \kappa)^2(a\epsilon)^2\eta_2, \quad (27)$$

where

$$\eta_1 = \int_0^\pi \sin^2(\alpha)F(\alpha, \theta)d\theta d\alpha, \quad (28)$$

$$\eta_2 = \int_0^{2\pi} \cos^2(p\theta)F(\alpha, \theta)d\theta d\alpha, \quad (29)$$

which after inserted in Eq. (24) result in

$$\overline{V_{n+1}^2} - \overline{V_n^2} = \eta_1(\kappa^2 - 1)\overline{V_n^2} + \frac{1}{2}(1 + \kappa)^2(a\epsilon)^2\eta_2. \quad (30)$$

Considering the approximation of continuous limit  $\overline{G_{n+1}} - \overline{G_n} \approx dG(n)/dn$ , we found a solution for the mean quadratic speed,

$$\overline{V^2} = \Psi + (V_0^2 - \Psi)e^{\eta_1(\kappa^2-1)n}, \quad (31)$$

where

$$\Psi = \frac{(a\epsilon)^2}{2} \frac{\eta_2}{\eta_1} \left( \frac{1 + \kappa}{1 - \kappa} \right).$$

To compare with the previous numerical simulations, we need to average over the ensemble of velocities and the history of velocities of all particles. Then, we need to average the previous instantaneous mean along the history of all quadratic means, i.e.,

$$\overline{V^2} = \frac{1}{n+1} \sum_{i=0}^n \overline{V_i^2}. \quad (32)$$

Provided that the arguments of the exponential are negative, their summation converges to

$$\sum_{i=0}^n e^{\eta_1(\kappa^2-1)i} = \left[ \frac{1 - e^{(n+1)\eta_1(\kappa^2-1)}}{1 - e^{\eta_1(\kappa^2-1)}} \right]. \quad (33)$$

Replacing Eq. (33) in (31) and then Eq. (31) in (32), we obtain

$$\overline{V^2} = \Psi + \left( \frac{V_0^2 - \Psi}{n+1} \right) \left[ \frac{1 - e^{(n+1)\eta_1(\kappa^2-1)}}{1 - e^{\eta_1(\kappa^2-1)}} \right]. \quad (34)$$

The final expression that describes the root mean square speed evolution is

$$V_{rms} = \sqrt{\Psi + \left( \frac{V_0^2 - \Psi}{n+1} \right) \left[ \frac{1 - e^{(n+1)\eta_1(\kappa^2-1)}}{1 - e^{\eta_1(\kappa^2-1)}} \right]}, \quad (35)$$

which corresponds to the continuous line (blue) in Figs. 2(a) and 2(b) in excellent agreement with the numerical results for the analyzed cases.

To conclude this analytical approach, we consider a few relevant limit cases for Eq. (35) that give us relevant insight into the overall

behavior of the obtained solution. When  $n = 0$ , we have

$$V_{rms} = V_0, \quad (36)$$

and for  $n \rightarrow \infty$ , we obtain the finite stagnation value

$$V_{rms} = a\epsilon \sqrt{\frac{1}{2} \frac{\eta_2}{\eta_1} \left( \frac{1 + \kappa}{1 - \kappa} \right)}. \quad (37)$$

Finally, we consider the intermediate values of  $n$  for small initial speeds  $V_0 \ll \sqrt{\Psi}$ . In the limit of  $\kappa \approx 1$ , we can expand to a first order exponential denominator in Eq. (35), while the numerator is taken to a second order due to the factor  $n + 1$  that contributes further to its nonlinearity. After a short algebra, we obtain

$$V_{rms} \cong a\epsilon \sqrt{\frac{\eta_2}{2} (1 + \kappa)(n + 1)}, \quad (38)$$

which for  $n \gg 1$  can be approximated to

$$V_{rms} \cong a\epsilon \sqrt{\frac{\eta_2}{2} (1 + \kappa)n^{1/2}}, \quad (39)$$

which leads to the observed growth rate in the numerical treatment of the system and also depends on the boundary oscillation amplitude, the angle distribution contained in  $\eta_2$ , and the restitution coefficient  $\kappa$ .

## V. CONNECTION WITH THERMODYNAMICS

As a final remark, we present an analogy between dynamical diffusion and the stagnation of the mean quadratic speed with the concept of thermalization. We start by borrowing the concept of temperature in a gas of noninteracting particles inside a closed region as being proportional to the mean of the quadratic peculiar velocities, which, in our case, is simply the mean of the quadratic velocities because the mean velocity of the gas is zero. In this sense, high temperatures are linked with high speeds, while the opposite is also true.<sup>18</sup>

We consider the diffusion process in the velocity space  $(V_x, V_y)$  to understand how the ensemble modify with collision. In order to characterize such diffusion, we evolve an ensemble of  $10^6$  particles in the velocity space, where each one started with the same velocity at some point in a circle with radius  $V_0 = 0.5$  and random angular position in the billiard.

Figures 5(a)–5(d) show the  $(V_x, V_y)$  space after 10, 25, 1000, and 10 000 collisions, respectively. The color scale measures the density of particles. Note that after 10 collisions [see Fig. 5(a)], the velocities become distributed around the original circle of radius  $V_0 = 0.5$ , where the density continues to be higher while some particles evolve towards the zero speed until the particles start populating the velocities near “zero.” This behavior is in agreement with the previous discussion of the initial plateau discussed in Sec. III [see Fig. 2(a)]. After 25 collisions, the velocities are more spread out and the average radius of the distribution grows, in agreement with the mean speed growth observed when the speed distribution becomes asymmetrical. Finally, after 1000 and 10 000 collisions, the distribution does not change much, which, expectedly, corresponds to the stagnation state, for which the individual velocity fluctuations do not affect the distribution function [see Fig. 3(a)].

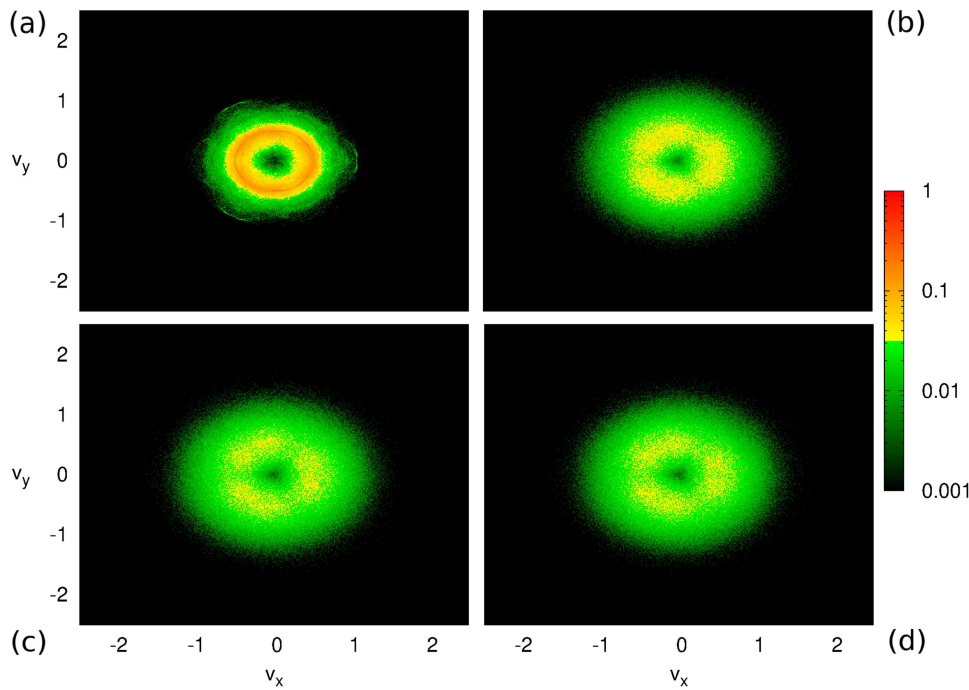


**FIG. 5.** Plot of the diffusion speed in the velocity space after (a) 10 collisions, (b) 25 collisions, and (c) 1000 collisions, and (d) 10 000 collisions for an ensemble of  $10^6$  particles with random positions and locations but with the same initial speed  $V_0 = 0.5$ . The logarithmic scale of colors represents the density of velocity in the velocity space, where the most dense regions are shown in red, while the less are in black.

It is interesting to notice that the velocity fluctuations are responsible to change the mean value of the ensemble of velocities in the space  $(V_x, V_y)$ , where these fluctuations might be estimated as the measure of the variance,

$$\sigma_v^2 = \langle \vec{v}^2 \rangle - \langle \vec{v} \rangle^2, \tag{40}$$

where the mean velocity  $\langle \vec{v} \rangle$  is “zero” because the particles are inside a nontranslating closed billiard, while the same does not apply for  $\langle \vec{v}^2 \rangle$ , which can be identified as Eq. (31).

Given that we know how the diffusion process in the system is, we can define an analogous quantity to the temperature named “dynamical temperature”  $T_d$ , which takes into account the characteristics of the dynamical system studied. This quantity can be written as

$$T_d \propto \overline{V^2}, \tag{41}$$

where the equality comes after the introduction of a suitable constant  $K_d$ , which leads us to

$$T_d = \frac{m}{2K_d} \left[ \Psi + (V_0^2 - \Psi) e^{\eta(\kappa^2 - 1)n} \right], \tag{42}$$

with  $m$  being the mass of each particle and  $K_d$  plays the role of the Boltzmann constant in our dynamical ensemble.

Figure 6 shows the numerical evolution of the dynamical temperature  $T_d$  as a function of the number of collisions  $n$ , for two restitution parameters close to “one.” As can be seen, when the initial speed  $V_0$  is less than  $\Psi$ , the dynamical temperature of the gas increases with the collisions until it reaches the stagnation regime, where it remains for the rest of the simulation. The stagnation regime in our context is analogous to system thermalization with a heat reservoir at constant temperature  $T_{sta}$ , which emerges from the interplay between the oscillating boundary and the inelastic collisions.

Provided there are no additional potentials acting inside the billiard, the particle energy is purely kinetic  $U_{tot} = E_k$  so that we can use the dynamical temperature to recast the total energy in terms of it,

$$\begin{aligned} U_{tot} &= E_k, \\ U_{tot} &= \frac{1}{2} Nm \overline{V^2}, \\ U_{th} &= NK_d T_d, \end{aligned} \tag{43}$$

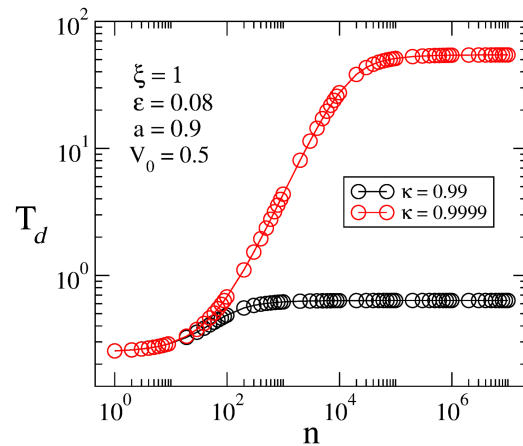


**FIG. 6.** Plot of evolution of the dynamical temperature for a gas of noninteracting particles in a time-dependent oval billiard in a function of the number of collisions.

where  $N$  is the number of particles. Expectedly, due to the definition of dynamical temperature, we recover an energy equation analogous to an ideal gas at temperature  $T_d$ .

## VI. CONCLUSIONS

In this paper, we have studied the evolution regimes of an ensemble of noninteracting particles in an oscillating billiard with collision losses. The evolution of the root mean square speed of the ensemble was determined both numerically and analytically. The analytical treatment was based on the diffusion process in the velocity space and resulted in a consistent description of all the regimes of the system evolution with considerable accuracy. The velocity plateau occurs due to the relaxation of the initial configuration. Then, for small initial velocities, the energy grows with a characteristic exponent close to  $1/2$ , characteristic of normal diffusion; otherwise, it will decrease exponentially for velocities larger than the saturation speed. Finally, the ensemble reaches a stagnation state independent of the initial configuration.

The stagnation regime is analogous to a thermalized state, where the distribution function becomes stationary and its temperature can be used to characterize the energy reservoir, here encompassing the vibrating boundary and the restitution constant. A dynamical temperature was defined to make a connection with thermodynamics that resulted in analogous equations for the energy of an ideal gas in an actual thermal system.

## ACKNOWLEDGMENTS

M.H. and D.C. acknowledge financial support by the Coordenação de Aperfeiçoamento de Pessoal de Nível Superior—Brasil

(CAPES) (Finance Code No. 001). I.L.C. and E.D.L. thank CNPq (Grant Nos. 300632/2010-0 and 303707/2015-1) and the São Paulo Research Foundation (FAPESP) (Grant Nos. 2018/03211-6 and 2017/14414-2) for their financial support.

## REFERENCES

- <sup>1</sup>A. Loskutov, A. B. Ryabov, and L. G. Akinshin, *J. Phys. A* **33**, 7973 (2000).
- <sup>2</sup>F. Lenz, F. K. Diakonov, and P. Schmelcher, *Phys. Rev. Lett.* **100**, 014103 (2008).
- <sup>3</sup>E. D. Leonel and L. A. Bunimovich, *Phys. Rev. Lett.* **104**, 224101 (2010).
- <sup>4</sup>E. Fermi, *Phys. Rev.* **75**, 1169 (1949).
- <sup>5</sup>S. O. Kamphorst and S. P. de Carvalho, *Nonlinearity* **12**, 1363 (1999).
- <sup>6</sup>R. E. de Carvalho, F. C. de Souza, and E. D. Leonel, *J. Phys. A Math. Gen.* **39**, 3561 (2006).
- <sup>7</sup>B. Batistić, *Phys. Rev. E* **90**, 032909 (2014).
- <sup>8</sup>V. Gelfreich and D. Turaev, *J. Phys. A* **41**, 212003 (2008).
- <sup>9</sup>V. Gelfreich, V. Rom-Kedar, and D. Turaev, *Chaos* **22**, 033116 (2012).
- <sup>10</sup>M. Hansen, D. Ciro, I. L. Caldas, and E. D. Leonel, *Europhys. Lett.* **121**, 60003 (2018).
- <sup>11</sup>E. D. Leonel, M. V. C. Gália, L. A. Barreiro, and D. F. M. Oliveira, *Phys. Rev. E* **94**, 062211 (2016).
- <sup>12</sup>H. Goldstein, C. P. Poole, and J. L. Safko, *Classical Mechanics* (Pearson, 2002).
- <sup>13</sup>E. D. Leonel, D. F. M. Oliveira, and A. Loskutov, *Chaos* **19**, 033142 (2009).
- <sup>14</sup>Noninteger numbers produce open billiard leading to escape of particles through the hole on the border.
- <sup>15</sup>A. J. Lichtenberg, M. A. Lieberman, and R. H. Cohen, *Physica D* **1**, 291 (1980).
- <sup>16</sup>D. F. M. Oliveira, M. R. Silva, and E. D. Leonel, *Physica A* **436**, 909 (2015).
- <sup>17</sup>A. Spanos, *Probability Theory and Statistical Inference* (Cambridge University Press, New York, 1999).
- <sup>18</sup>F. Reif, *Fundamentals of Statistical and Thermal Physics* (Waveland Press, 2009).